Cousin *et al. Molecular Cancer* (2024) 23:197
https://doi.org/10.1186/s12943-024-02092-x

Molecular Cancer

CORRESPONDENCE Open Access

Identification of microenvironment features associated with primary resistance to anti-PD-1/PD-L1 + antiangiogenesis in gastric cancer through spatial transcriptomics and plasma proteomics

Sophie Cousin[1†], Jean-Philippe Guégan[2†], Kohei Shitara[3], Lola Jade Palmieri[1,2], Jean Philippe Metges[4], Simon Pernot[1], Shota Fukuoka[5], Shohei Koyama[5], Hiroyoshi Nishikawa[5], Carine A. Bellera[6,7], Antoine Adenis[8], Carlos A. Gomez-Roca[9], Philippe Alexandre Cassier[10], Antoine Hollebecque[11], Coralie Cantarel[6,7], Michèle Kind[12], Isabelle Soubeyran[13], Lucile Vanhersecke[13], Alban Bessede[2] and Antoine Italiano[1,10,14*]

Abstract

Anti-angiogenic agents elicit considerable immune modulatory effects within the tumor microenvironment, underscoring the rationale for synergistic clinical development of VEGF and immune checkpoint inhibitors in advanced gastric cancer (AGC). Early phase studies involving Asian patients demonstrated encouraging anti-tumor efficacies. We report the results of the REGOMUNE phase II study, in which Caucasian patients were administered regorafenib, a multi-tyrosine kinase inhibitor, in combination with avelumab, a PD-L1-targeting monoclonal antibody. This therapeutic regimen resulted in deep and durable responses in 19% of patients, with the median duration of response not yet reached. Notwithstanding, a significant proportion of AGC patients exhibited no therapeutic advantage, prompting investigations into mechanisms of inherent resistance. Comprehensive biomarker profiling elucidated that non-responders predominantly exhibited an augmented presence of M2 macrophages within the tumor microenvironment and a marked overexpression of S100A10 by neoplastic cells, a protein previously implicated in macrophage chemotaxis. Additionally, peripheral biomarker assessments identified elevated levels of cytokines, including CSF-1, IL-4, IL-8, and TWEAK, correlating with adverse clinical outcomes, thereby accentuating the role of macrophage infiltration in mediating resistance. These insights furnish an invaluable foundation for elucidating, and potentially circumventing, resistance mechanisms in current AGC therapeutic paradigms, emphasizing the integral role of tumor microenvironmental dynamics and immune modulation.

†Sophie Cousin and Jean-Philippe Guégan contributed equally to this work.

*Correspondence:
Antoine Italiano
a.italiano@bordeaux.unicancer.fr

Full list of author information is available at the end of the article

Introduction

Recently, a new standard of care for several cancers, including advanced gastric cancer (AGC), has emerged in the form of immune checkpoint inhibitors (ICIs) like anti-programmed cell death-1 (PD-1) or programmed cell death ligand-1 (PD-L1) monoclonal antibodies. In AGC treatment, nivolumab, an anti-PD-1 monoclonal antibody, has been instrumental in improving survival outcomes as per the pivotal phase III trials such as the ATTRACTION-2 study in Asia for third-line or subsequent treatments [1], and the global CheckMate-649 study [2] for first-line treatment combined with standard cytotoxic agents. The response rate in first-line treatment for patients with HER2-positive AGC improved significantly when pembrolizumab was added to trastuzumab and chemotherapy, as demonstrated in the phase III KEYNOTE-811 study [3]. However, it is important to note that a significant proportion of AGC patients exhibited resistance to ICIs, underlining the need to develop additional combined immunotherapies.

Previous studies have shown that the inhibition of the VEGF pathway can stifle tumor growth and curb immune-suppressive cell infiltration like tumor-associated macrophages, regulatory T cells, and myeloid-derived suppressor cells while promoting the mature dendritic cell fraction [4]. In an in vivo model, multikinase inhibitors of VEGF receptors and other receptor tyrosine kinases dramatically reduced immune-suppressive cells, thereby enhancing the antitumor activity of PD-1 inhibitors [5].

Prior early phase studies, conducted exclusively with Japanese patients, showcased promising antitumor activity when anti-PD-1 antibodies were paired with multikinase inhibitors such as regorafenib plus nivolumab (REGONIVO) [6] or lenvatinib plus pembrolizumab (LENPEM) [7] in the treatment of AGC. However, a substantial percentage of patients remain unresponsive to these therapeutic combinations.

The REGOMUNE trial represents the first phase 2 study that delves into the efficacy of a therapeutic strategy that pairs immune checkpoint inhibition with the multityrosine kinase inhibitor, regorafenib, in Caucasian patients diagnosed with AGC. This study not only reports the findings from the REGOMUNE trial but also integrates comprehensive correlative analyses using samples from both the REGOMUNE and REGONIVO studies. These analyses are designed to identify mechanisms of primary resistance to the combination of ICIs and tyrosine kinase inhibitors in AGC.

Patients and methods

REGOMUNE study design and participants

The REGOMUNE trial was a phase II, single-arm, multicenter basket study conducted across four locations in France. This study enrolled participants from the gastric cancer cohort who were at least 18 years of age and had histologically confirmed advanced or metastatic gastric cancer. Eligible patients were required to have an Eastern Cooperative Oncology Group performance status between 0 and 1, measurable disease as per RECIST 1.1 standards, at least one prior round of systemic treatment, and satisfactory hematological, renal, metabolic, and hepatic functions. A detailed list of the eligibility criteria can be found in the study protocol (see Supplementary Data). Participants underwent a comprehensive blood test that assessed variables including blood cell count, alanine aminotransferase, aspartate aminotransferase, alkaline phosphatase, albumin, bilirubin, lipase, creatinine phosphokinase, coagulation, creatinine, and urea nitrogen levels. Key exclusion criteria were previous treatment with avelumab or regorafenib, anti–PD-1, anti–PD-L1, anti–PD-L2, anti-CD137, or anti-cytotoxic T-lymphocyte–associated antigen-4 antibodies, with the full list detailed in the protocol. The REGOMUNE study was executed in adherence with the principles of the Declaration of Helsinki. The trial protocol, including a review of the risks and benefits to the study participants, was approved by a Central Institutional Review Board (Comité de Protection des Personnes Sud-Est II, Lyon, France), as mandated by French regulations. Informed consent was obtained in writing from all participating patients.

Once eligibility was confirmed, patients embarked on a treatment regimen that included regorafenib (160 mg per day) administered on a schedule of three weeks on and one week off, across 28-day cycles. From day 15 of cycle 1, avelumab was introduced and administered biweekly as an intravenous infusion at a dose of 10 mg/kg. Treatment continued until the progression of the disease, the occurrence of intolerable side effects, the decision by the investigator to cease treatment, or the withdrawal of patient consent. Regular follow-up assessments were conducted to monitor any adverse events, which were then graded based on the NCI Common Terminology Criteria for Adverse Events (CTCAE) version 5.0. Baseline laboratory assessments were carried out and subsequently performed every two weeks until treatment discontinuation.

Regorafenib dosage adjustments were permitted to manage any adverse events (as detailed in the study protocol). The dosage could be reduced first to 120 mg and then further to 80 mg as required, based on the clinical situation. If patients required a delay exceeding four weeks from the last dose of regorafenib, they were required to discontinue regorafenib permanently but could continue with avelumab if deemed appropriate. Unlike regorafenib, dose reduction of avelumab was not allowed, though dosage interruptions based on the

severity of immune-related adverse events were permitted. Patients who needed two or more consecutive cancellations of avelumab injection were required to discontinue avelumab permanently, but they could continue with regorafenib.

Tumor lesions were evaluated according to RECIST version 1.1, at baseline (within four weeks prior to cycle 1 day 1) and every eight weeks thereafter until disease progression or commencement of another treatment. For all consenting patients, tumor samples were collected at baseline and on day 1 of cycle 2. These samples were analyzed to evaluate the impact of the treatment on the tumor microenvironment and identify potential biomarkers associated with treatment outcomes.

Outcomes

The primary endpoint of this study was the 6-month objective response rate, defined as the proportion of patients exhibiting an objective response (whether confirmed or unconfirmed) to the treatment, based on an adaptation of RECIST 1.1 guidelines and subject to centralized radiological review.

Secondary endpoints comprised the best overall response, 6-month objective response rate, 6-month progression-free rate, 1-year progression-free survival (PFS), 1-year overall survival (OS), and safety. The best overall response was identified as the most favorable response at any given time point throughout the treatment. PFS was calculated as the duration from the initiation of the study treatment to the first instance of disease progression or death from any cause. OS was defined as the time elapsed from the commencement of the study treatment to death from any cause. Safety was evaluated and graded according to the common toxicity criteria outlined in the NCI's CTCAE v5.0.

Spatial transcriptomics

Slides were prepared for the Nanostring Whole Transcriptome Atlas (WTA) assay according to Nanostring's instructions (MAN-10150-03). After baking the slides for 1 h at 62 °C, slides were loaded onto the Ventana Discovery for paraffin removal, rehydration, heat-induced epitope retrieval (CC1 for 32 min at 99 °C) and enzymatic digestion (1 µg/ml proteinase K for 16 min at 37 °C). The tissue sections were then hybridized overnight with the oligonucleotide probe mix (Human WTA panel). Following 2×5 min stringent washes (1:1 4x SSC buffer & formamide), the slides were blocked and then incubated with the following morphology marker antibodies: PanCK (AE1+AE3, 532 channel, Novus Biologicals) and CD45 (2B11+PD7/26, 594 channel, Novus Biologicals). Syto 13 (488 channel, Invitrogen) was used as a nuclear stain. Tissue sections were then loaded into the GeoMx platform and Regions of interest (ROIs) were selected on mixed tumor-stroma areas (Supplementary Fig. 1). ROIs were further segmented in CD45+and PanCK+areas of illumination (AOIs), to separate immune from tumor cells. UV light was then directed by the GeoMx at each AOI to release and collect the RNA ID and UMI-containing oligonucleotide tags from the WTA probes. Illumina i5 and i7 dual indexing primers were added to the oligonucleotide tags during PCR (4 µL of collected oligonucleotides/AOI) to uniquely index each AOI. AMPure XP beads (Beckman Coulter) were used for PCR purification. Library concentration was measured using a Qubit fluorometer (Thermo Fisher Scientific) and quality was assessed using a Tapestation 4150 (Agilent). Sequencing was finally performed on an Illumina NovaSeq6000 and fastq files were processed by the NanoString DND pipeline, resulting in count data for each WTA probe in each AOI. After quality check of the probes and AOIs according to Nanostring's standards, raw counts were normalized using quantile normalization from GeomxTools R package (version 3.0.1) and differentially expressed genes was analyzed using limma with patient ID as blocking factor. A fold change≥2 and an adjusted p value≤0.05 were used as cut-off values. To estimate the cell abundances in each AOIs, SpatialDecon (version 1.6.0) algorithm was used using the safeTME as cell profile matrix. M2 activation gene signature (https://doi.org/10.3390/cancers14051290) was tested on normalized data using the fgsea R package (version 1.22.0). Go-term enrichment was analyzed using fgsea R package (v1.22.0) and rrvgo (v1.14.0).

Multiplex immunohistofluorescence (mIHF)

Multiplexed immunohistofluorescence was performed on the Ventana Discovery platform (Roche, Ventana) using two different panels: panel (1) CD8 / CD11b / CD68 / HLA-DR / PanCK / DAPI and panel (2) S100A10 / PanCK / DAPI. The following antibodies were used: CD8 (C8/144B, Dako), CD11b (EPR1344, Abcam), CD68 (PG-M1, Dako), HLA-DRA (E9R2Q, Cell Signaling Technology), S100A10 (4E7E10, Cell Signaling Technology) and PanCK (AE1/AE3/PCK26, Ventana). Bound primary antibodies were detected using OmniMap anti-Rb HRP (760–4311, Ventana) and OmniMap anti-Ms HRP (760–4310, Ventana) detection kits followed by TSA opal fluorophores (Opal 480, Opal 520, Opal 570, Opal 620, Opal 690 and/or Opal 780, Akoya Bioscience). The following combinations were used: (1) CD8 – Opal 520 / CD68 – Opal 620 / CD11c – Opal 480 / CD11b – Opal 570 / HLA-DR – Opal 690 / PanCK – Opal 780; (2) S100A10 – Opal 520 / PanCK – Opal 780. The slides were counterstained with spectral DAPI (Akoya Bioscience) and cover-slipped. The slides were scanned using the PhenoImager HT System (Akoya), and the multispectral images obtained were unmixed using spectral libraries

that were previously built from images stained for each fluorophore (monoplex), using the inForm Advanced Image Analysis software (inForm 2.6.0, Akoya Bioscience) combined with Opal detection kit (Akoya Bioscience). Tumor areas were delineated in PhenoChart (Akoya Bioscience) and analyzed using inForm software (Akoya Bioscience, version 2.6.0) to first segment the tissue in tumor and stroma areas according to PanCK staining. Cell segmentation was achieved using an object-based approach implemented in inForm software. DAPI staining identified cell nuclei, while additional membrane marker staining refined the segmentation of individual cells. The mean marker intensity was extracted for each cell and signal intensities were further normalized using the GaussNorm function from flowstat R package. Cells were finally phenotyped using a thresholding method in FlowJo (version 10.8.0).

PD-L1 scoring

Slides were stained with the PD-L1 antibody by immunochemistry using the QR-1 antibody clone (Diagomics). In brief, stainings were performed on the Ventana Discovery platform (Roche, Ventana) with the protocol RUO discovery universal according to the manufacturer's recommendations with the detection kits OmniMap anti-Rb HRP (760–4311, Ventana). The slides were scanned using the PhenoImager HT system (Akoya) and PD-L1 status was determined with the Combined Positive Score (CPS) following established guidelines. For this purpose, all PD-L1-positive cells were considered, including viable tumor cells, lymphocytes, and macrophages, relative to the total number of tumor cells. Only complete or partial membranous staining was considered, but not cytoplasmic staining.

Plasma proteomics

Plasma proteomic analysis has been carried out thanks to the Olink Proximity Extension Assay (PEA) (Olink Proteomics AB, Uppsala, Sweden). In brief, when pairs of oligonucleotide-labeled antibody probes bind to their targeted protein, oligonucleotides will hybridize in a pair-wise manner, generating an unique DNA reporter sequence which can be amplified by real-time PCR. Plasma samples were assessed using the Olink® Target 96 Immuno-Oncology panel (Olink Proteomics AB, Uppsala, Sweden) according to the manufacturer's instructions and quantified using a microfluidic real-time PCR instrument (Biomark HD, Fluidigm). Data were quality controlled and normalized using the IPC method (Olink NPX Signature). The final assay read-out is presented in NPX values, which is an arbitrary unit on a log2-scale where a high value corresponds to a higher protein expression. All assay validation data (detection limits, intra- and inter-assay precision data, etc.) are available on manufacturer's website (www.olink.com).

Survival analysis

The log-rank test was used to compare Kaplan–Meier survival curves (survival R package v3.3.1). The Cox proportional hazards regression model was used to estimate hazard ratios (HRs) and 95% confidence intervals (CIs). Patients were classified as "High" or "Low" based on an optimized threshold obtained using the maximally selected rank statistics from the maxstat R package and using PFS as the optimal outcome (survminer R package v0.4.9). All analyses were conducted using R v.4.2.1.

Role of the funding source

The study was sponsored by Institut Bergonié, Comprehensive Cancer Center (Bordeaux, France). The data were collected with the sponsor data management system and were analyzed and interpreted by representatives of the sponsor in collaboration with the investigators. S. Cousin, C. Cantarel, C. Bellera, and A. Italiano had access to the raw data. The corresponding author had full access to all the data in the study and had final responsibility for the decision to submit for publication.

Data sharing

Individual participant data that underlie the results reported in this article will be available after deidentification upon publication and up to 6 years after article publication to researchers who provide a methodologically sound proposal. Requests should be sent to the corresponding author.

Results

Trial design and patients' characteristics

The REGOMUNE trial is a basket study comprising 17 concurrent, single-arm phase 2 trials, each designed to evaluate the efficacy and safety of regorafenib in conjunction with avelumab in distinct tumor types. For the gastric cancer cohort, the primary endpoint was the objective response rate (ORR). Secondary endpoints included progression-free survival (PFS), overall survival (OS), and safety. Eligible participants were those aged 18 years or older, with histologically confirmed sarcoma following a central review, an Eastern Cooperative Oncology Group Performance status of 0–1, and adequate renal, hepatic, and cardiac functions. Eligibility did not consider the type or number of prior treatments. Blood tests encompassed assessments of blood cell count, alanine transaminase (ALT), aspartate aminotransferase, alkaline phosphatase, albumin, bilirubin, creatinine, and urea nitrogen. A washout period of 21 days was required for previous systemic anticancer therapy. Key exclusion

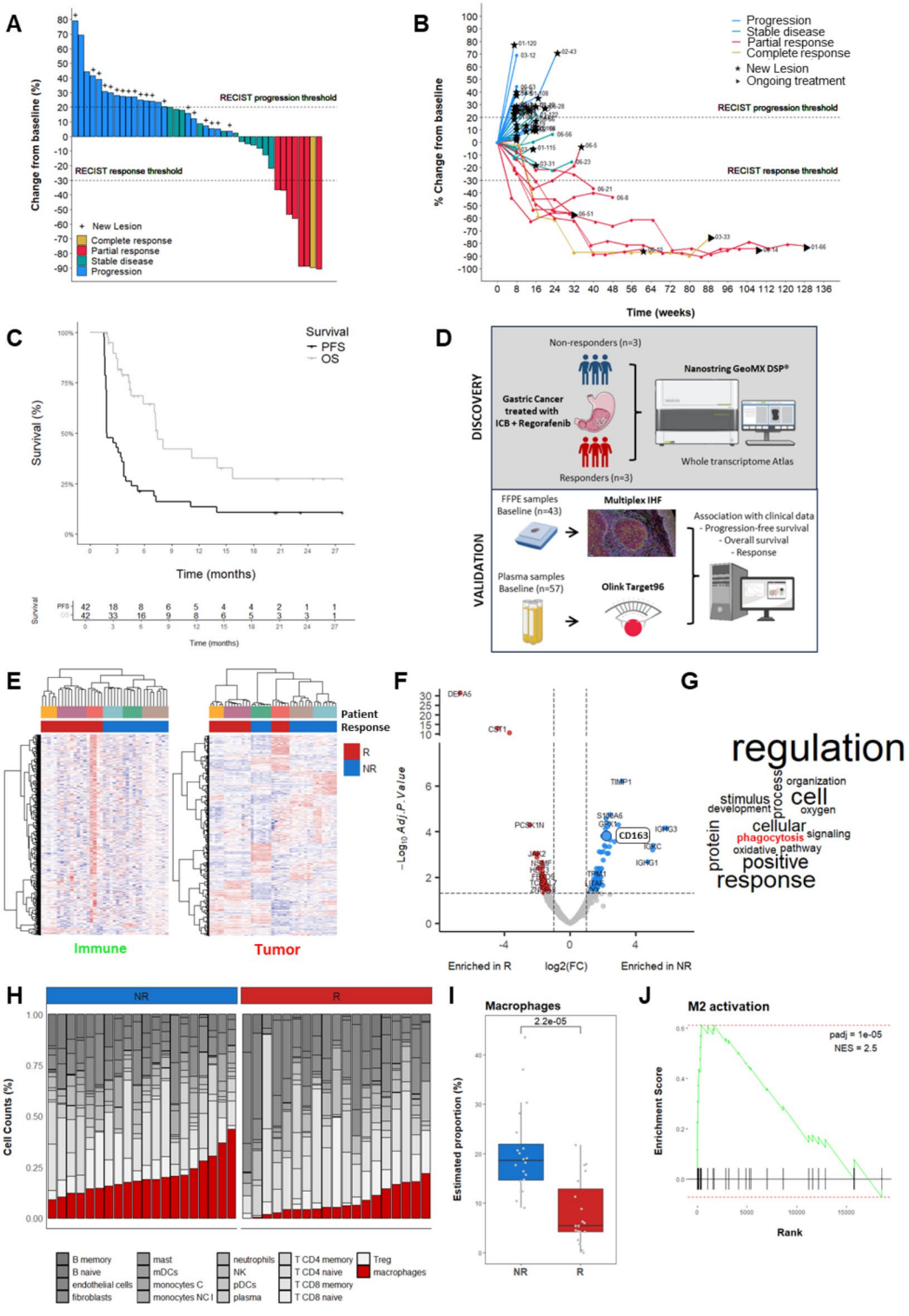

Fig. 1 (See legend on next page.)

(See figure on previous page.)

Fig. 1 Spatial transcriptomic unveils correlation of macrophages infiltration with primary resistance to the Regorafenib-Avelumab combination. (**A**) Waterfall plot and (**B**) Spider plot of the maximum change in tumor size in patients with gastric cancer treated with regorafenib plus avelumab and eligible for efficacy ($n=42$). (**C**) Kaplan-Meier curves of the progression-free survival and overall survival. (**D**) Flow chart illustrates the strategy used to identify biomarkers linked with resistance to the Regorafenib-Avelumab combination within a discovery cohort. This strategy is further assessed in a validation cohort. (**E**) ROIs from the "Tumor" and "Immune" sections underwent unsupervised clustering. (**F**) A volcano plot showcases the differential gene expression between patients who responded (R) and those who didn't (NR) in the "Immune" section. The gene CD163 is notably more prevalent in NR patients. (**G**) A word cloud provides a concise overview of the Gene Ontology (GO) enrichment analysis. (**H**) A histogram indicates the estimated immune cell populations derived from the GeoMX data deconvolution, using the SpatialDecon algorithm. The macrophages population stands out, marked in red. (**I**) The SpatialDecon algorithm estimates the proportion of Macrophages in both responder (R) and non-responder (NR) patients. A Wilcoxon test was used to determine the P-value. (**J**) The gene set enrichment analysis highlights the M2 activation signature within the "Immune" sections of the patient samples. RECIST = Response Evaluation Criteria in Solid Tumours

criteria included prior treatment with regorafenib and/or any anti-PD1/PDL1 monoclonal antibody.

Between 26th December 2018 and 26th March 2021, 49 patients were included in the study. Seven patients failed to meet the eligibility criteria for efficacy analysis, leaving 42 patients who were assessable for the primary endpoint. The baseline characteristics of the patients are detailed in Supplementary Table 1.

After a median follow-up 14.5 months (95% CI 4.4–20.7), four patients (13.3%) were still receiving treatment, and 45 patients (86.7%) discontinued treatment. Discontinuation was related to disease progression in 43 cases (73%), investigator decision for one patient (15.5%) and adverse event for one patient (11.5%) (Supplementary Fig. 2).

Efficacy

This study employed a Bayesian approach and adhered to an adaptive trial design, promoting more compact yet insightful trials, and facilitating decision making throughout the clinical trial. This strategy offers the advantage of enabling gradual knowledge acquisition as opposed to rigid trial designs with predetermined sample sizes, which often limit amendments. Throughout each efficacy analysis, the criteria for futility were never met, thus allowing the patient accrual to continue until reaching the maximum limit as per the protocol ($n=50$). However, recruitment was halted upon the inclusion of the 49th patient due to a decision by the sponsor, with the intention of accelerating. One patient had complete response, 7 patients had partial response, 12 patients had stable disease and 22 patients had progressive disease as per RECIST 1.1 criteria (Fig. 1A).

Responses were durable, with a median duration of response which was not reached at the time of analysis (Fig. 1B). Median PFS was 1.9 months % (95% CI, 1.8–3.2 months) (Fig. 1C). The 6-month and 1-year PFS rates were 21.4% (95% CI, 10.6–34.7%) and 18.8% (95% CI, 8.7–31.8%), respectively. Additionally, the median OS was 7.5 months (95% CI, 4.5–15.7 months), with the 6-month and 1-year OS rates at 64.4% (95% CI, 45.3–78.4) and 37.5% (95% CI, 19.1–55.9), respectively (Fig. 1C). The Growth Modulation Index (GMI), defined as the ratio of progression-free survival with the investigational regimen compared to the most recent prior line of therapy, was available for all the patients included in the efficacy analysis. Among them, 15 patients had a GMI > 1, indicating a clinical benefit compared to their most recent prior line of therapy.

Safety

Forty-nine patients, each having received at least one dose of regorafenib and/or avelumab, were assessed for safety. The treatment was generally well-tolerated. Treatment-related adverse events and laboratory abnormalities occurring in over 5% of patients for grades 1–2, and any instance for grades 3 and 4, are detailed in Supplementary Table 2. The most frequently encountered clinical treatment-related adverse events included fatigue, diarrhea, palmar-plantar erythrodysesthesia syndrome, anorexia, mucositis, and infusion-related reactions. As anticipated, the predominant treatment-related laboratory abnormalities were transaminitis and an increase in thyroid-stimulating hormone (TSH). Serious adverse events were reported in 26 patients, accounting for 53.1% of the study population. Adjustments in treatment due to drug-related adverse events were necessary for 30 patients (59.2%) with regorafenib (including 21 temporary discontinuations, 7 dose reductions, and 2 permanent discontinuations) and 18 patients (70%) with avelumab (with 1 resulting in permanent discontinuation). It is important to note that there were no reported deaths due to drug-related toxicity.

Exploratory analysis of biomarkers (REGOMUNE and REGONIVO studies)

Although the efficacy results were encouraging, a substantial proportion of patients enrolled in the REGOMUNE study did not display clinical benefit, similar to the observations in the REGONIVO study. We conducted an in-depth analysis of baseline biological samples from patients enrolled in these two studies to identify the determinants of the response to ICIs combined with multikinase tyrosine inhibitors in patients with AGC. First, we spatially profiled the expression of > 18,000 protein-coding genes across six tumors (three with objective

response and three with progressive disease as the best response) using the GeoMx whole-transcriptome atlas (WTA) (Fig. 1D). A first set of slides from baseline biopsies was stained with the panel CD45/PanCK/Sytox to visualize the tissue and to pre-select the regions of interest (ROIs) to be analyzed (Supplementary Fig. 1). For each slide, ROIs were drawn to analyze the expression of the WTA gene panel within the tumor region. Each tumor ROI was further segmented in 2 AOIs (area of illumination) based on the PanCK and CD45 staining to analyze the "Tumor" (PanCK+CD45-) and "Immune" (CD45+) compartments (Supplementary Fig. 1). The number of AOI for each patient group is summarized in the supplementary Table 3. Analysis of the top 25% variant genes between AOIs was performed separately in each compartment. Unsupervised data clustering showed a strong stratification of responder and non-responder patients with data collected from the immune compartment (Fig. 1E). Analysis of genes differentially expressed in immune regions identified the overexpression of CD163 gene in resistant patients (Fig. 1F – Supplementary Table 4). Consistently, Gene Ontology (GO) term enrichment analysis revealed a significant enrichment of terms associated with macrophage functions (Fig. 1G - Supplementary Fig. 3). We then performed immune cell deconvolution to estimate the relative abundancies of specific immune cell subsets between responder and resistant patients. Strikingly, M2 macrophage was the one significantly upregulated in the immune compartment of resistant patients (Fig. 1H-J). Comparative transcriptomic analysis of the tumor compartment between non-responders and responders revealed a strong upregulation of S100A10, a member of the S100 protein family, alongside its ligand, Annexin A2 in non-responder patients (Supplementary Fig. 4A - Supplementary Table 5). Notably, these two elements form a heterotetrameric complex playing a key role in regulating tumor cell proliferation, angiogenesis and macrophage recruitment. Of note, there was no significant difference in PD-L1 expression between responders and non-responders. We further confirmed the absence of an association between PD-L1 expression, as measured by the Combined Positive Score (CPS) through immunohistochemistry, and progression-free survival (PFS), overall survival (OS), and objective response (Supplementary Fig. 5).

To validate our findings and visualize the differences in immune cell abundances between responders and non-responders, we developed two multiplex IHF panels that enabled simultaneous detection of panel 1: CD8+T cells (CD8), M1 macrophages (CD11b+, CD68+, HLA-DR+), M2 macrophages (CD11b+, CD68+, HLA-DR-) (Fig. 2A-B), and tumor cells (PanCK); panel 2: S100A10, and tumor cells (PanCK) (Supplementary Fig. 4B). To corroborate the robustness of our findings and broaden the scope of our spatial transcriptomics methodology, we utilized these panels on all available whole-section baseline tumor biopsies from patients enrolled in the REGOMUNE and REGONIVO studies ($n=43$), as both studies explored the same strategy of pairing regorafenib with a PD1/PDL1 inhibitor. The detailed methods of the REGONIVO study were reported previously [6]. We confirmed M2 macrophages - as the immune cell population most differentially represented between responders and non-responders (Fig. 2C and F) and the ratio M2/M1 being significantly higher in patients displaying primary resistance (Fig. 2C and I). The median PFS and OS of patients with tumors highly infiltrated by CD68+HLA-DR- cells were 2.52 and 7.25 months versus 9.61 and 22.16 months for patients with low infiltration, respectively ($P=0.023$ and $P=0.067$, respectively) (Fig. 2D-E). Patients with a high M2/M1 ratio had also a worse PFS (2.59 vs. 11.28 months, $p=0.005$) and OS (7.4 vs. 22.16 months, $p=0.12$) than patients with a low M2/M1 ratio (Fig. 2G-H). High abundance of tumor cells expressing S100A10 was also associated with a trend for worse response (27.6% vs. 57.1%, $p=0.06$), PFS (2.72 vs. 7.56 months, $p=0.081$) and OS (7.46 vs. 13.48 months, $p=0.22$) (Supplementary Fig. 4).

To detect potential peripheral biomarkers associated with resistance to regorafenib plus ICI, we implemented a proteomics analysis of plasma samples from patients enrolled in the REGOMUNE and REGONIVO studies by using the Olink Target 96 Immuno-Oncology panel which rely on a qPCR readout. We found that several cytokines typically associated with macrophage infiltration such as CSF-1, IL-4, IL-8 and TWEAK were upregulated in patients with poor outcome (Fig. 3A) and significantly associated with M2 abundance detected in tissue (Fig. 3B). For instance, the PFS (Fig. 3C), OS (Fig. 3D) and objective response rates (Fig. 3E) were 1.78 versus 4.41 months ($P<0.001$), 7.2 versus 13.48 months ($P=0.009$) and 0% versus 43.2% ($p=0.003$) in the CSF-1high group compared with the CSF-1 low group, respectively.

Discussion

While ICI have brought about significant therapeutic advances, manifesting in sustained responses and improved survival rates across a variety of malignancies, their effectiveness in metastatic cancer contexts, especially in gastric and gastroesophageal junction cancer (GC/GEJC), remains limited. In the landscape of advanced and metastatic GC/GEJC, single-agent ICI has shown clinical benefits in patients with mismatch-repair/microsatellite instability high (MMR/MSI-H) phenotypes and in third-line treatment scenarios for patients with elevated PD-L1 expression [1, 8]. Yet, the therapeutic opportunities for the broader patient population remain

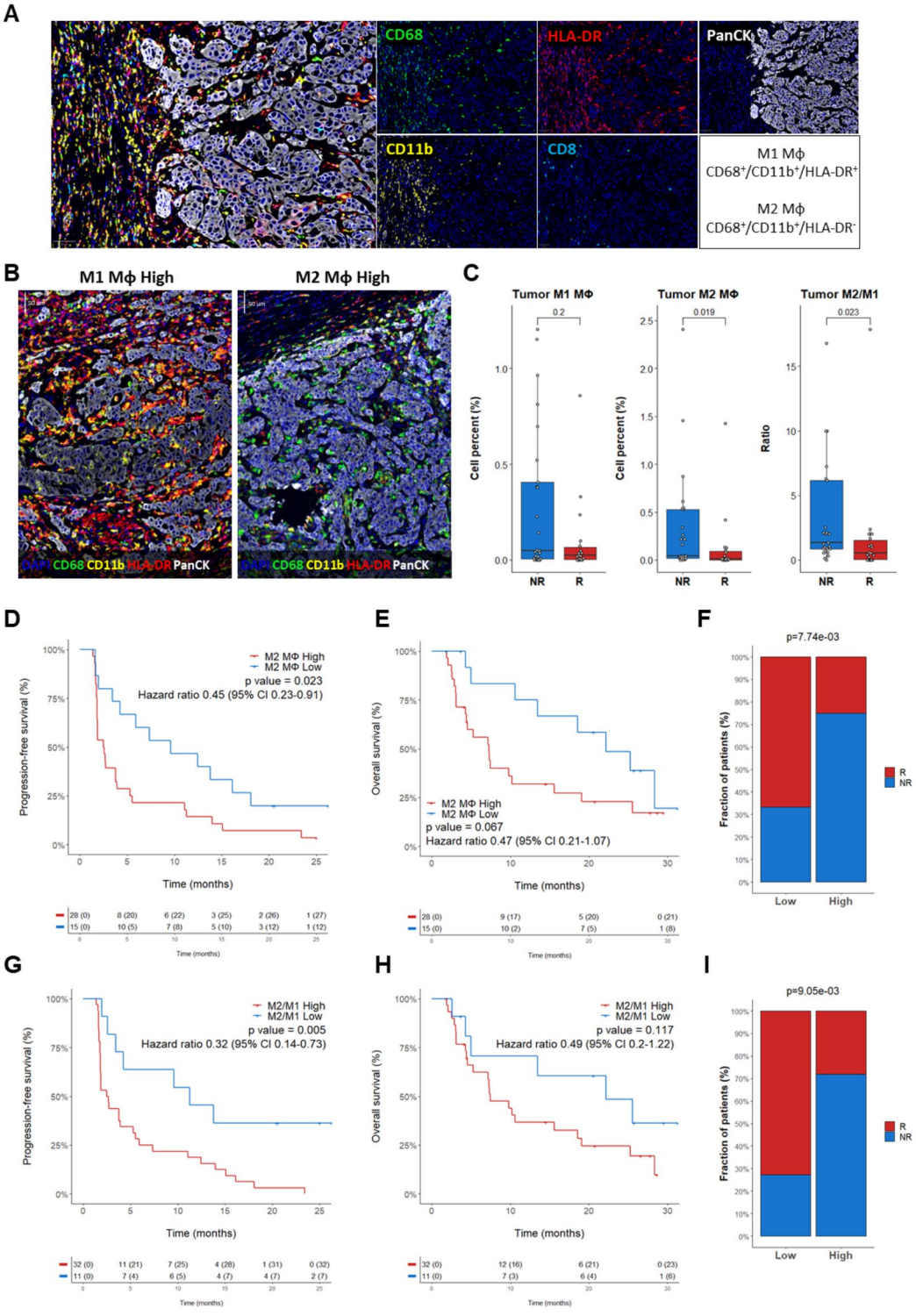

Fig. 2 Multiplex immunofluorescence analysis showed that M2 macrophages are enriched in non-responding patients to the regorafenib-avelumab therapy. (**A**) Representative gastric cancer sample stained with multiplex immunohistofluorescence (mIHF) for CD8, CD11b, CD68, HLA-DR, PanCK, and DAPI. M1 macrophages (M1 MΦ) were identified as CD68+/CD11b+/HLA-DR + cells, while M2 macrophages (M2 MΦ) were characterized as CD68+/CD11b+/HLA-DR- cells. (**B**) Illustration of patients with high levels of M1 (left) and M2 (right) macrophages. (**C**) Boxplot representation of the percentage of M1 macrophages, M2 macrophages, and the ratio of M2/M1 macrophages in responders (R) and non-responders (NR) among patients. (**D**-**E**) Kaplan-Meier curves depicting the progression-free survival of patients classified as "High" or "Low" based on their percentage of M2 macrophages (**D**) and for the M2/M1 ratio (**E**). (**F**) Response rates categorized by levels of M2 macrophages (**I**) Response rates based on the M2/M1 ratio (Chi-square test). (**G**-**H**) Kaplan-Meier curves illustrating the overall survival (OS) of patients classified as "High" or "Low" based on their percentage of M2 macrophages (**G**) and the M2/M1 ratio (H)

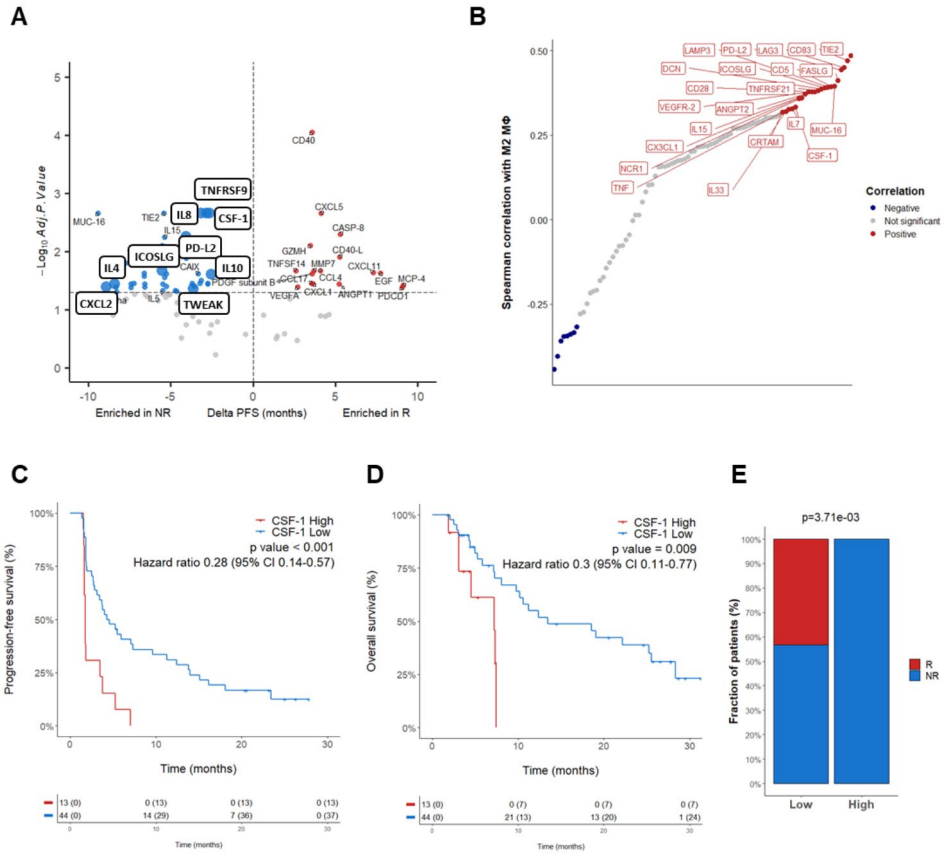

Fig. 3 Plasma Proteomic Analysis in patients enrolled in the REGOMUNE and REGONIVO studies using the Olink Immuno-Oncology Target96 panel. (**A**) Volcano plot illustrating the differential expression of cytokines in patients responding (R) versus not-responding (NR) to the Regorafenib-anti-PD1/PD-L1 treatment. (**B**) Spearman correlation analysis showing the relationship between M2 macrophage levels determined by immunohistofluorescence and the cytokine levels quantified. (**C**) Kaplan-Meier survival curve demonstrating the progression-free survival rates of patients categorized as "High" or "Low" based on their plasma levels of CSF-1. (**D**) Kaplan-Meier survival curve displaying the overall survival rates of patients classified as "High" or "Low" based on their plasma levels of CSF-1. (**E**) Response rates based on CSF-1 plasma levels. Statistical significance was assessed using a Chi-squared test

narrow. Consequently, emerging research is focusing on developing combinatorial approaches to enhance IO responsiveness. Notably, integrating ICI with other systemic therapeutic modalities, especially molecularly targeted agents, is a subject of intense investigation.

The REGOMUNE study's results reinforce that combining VEGFR TKIs with checkpoint inhibitors can lead to a sustained response in a segment of patients with AGC. Noteworthy is the synergy between regorafenib and avelumab for chemoresistant gastric cancer, which attained an ORR of 19% a significant improvement from the mere 3% seen with solo regorafenib in the INTEGRATE study [9]. These findings are consistent with previous early phase studies that demonstrated response rates ranging between 20 and 44% for VEGR/PD1 or PDL1 combinations in Asian patients with chemo-refractory ADG [7, 10, 11]. However, a major caveat remains: a significant number of patients do not respond to PD1/PDL1 combined with VEGFR inhibition. Despite PD-L1 CPS being acknowledged as an outcome predictor in advanced gastroesophageal cancer, its predictive potential was not validated in our study or other investigations exploring this combination [6].

Our in-depth analysis of tumor samples, employing high-throughput spatial transcriptomics, multiplexed IHF, and plasma proteomics, indicated that the primary resistance to the combined therapy of PD1/PD-L1 and VEGFR inhibition is associated with a unique tumor microenvironment. Through unsupervised clustering of spatial transcriptomics data, a clear clustering emerged that differentiated responder and resistant patients based on the gene expression profiles within the immune compartment. This underscored the crucial role of the tumor microenvironment in determining the probability of response to VEGFR/PD1 inhibition in AGC. We showed that this environment was characterized by an abundance of M2 macrophages and elevated levels of circulating cytokines that foster monocyte recruitment, differentiation, and a shift towards an M2-like protumoral phenotype. Pre-clinical studies indicated that these

immunosuppressive macrophages play a pivotal role in resisting anti-PD-1 therapies in gastric cancer [12]. We previously reported the significant role of M2 macrophages in resistance to regorafenib combined with avelumab in patients with advanced MSS colorectal cancer [13]. While our findings on M2-like macrophage enrichment in non-responders are insightful, future studies should use more nuanced approaches, Indeed, the M1/M2 dichotomy is an oversimplification of the dynamic and heterogeneous nature of macrophage phenotypes observed in vivo. However, the results from our study suggest that merely combining VEGFR inhibitors with anti-PD1/PDL1 inhibitors is insufficient to counteract the resistance posed by the presence of TAMs in the microenvironment of AGC.

Our comparative transcriptomic analysis further highlighted the upregulation of S100A10 in resistant patients, a member of the S100 protein family. Confirming this, our IHF experiments showed a significantly worse prognosis in patients with overexpressed S100A10. This protein has been identified as one of the top up-regulated genes in gastric cancer compared to normal gastric epithelia and plays a crucial role in the recruitment of tumor-promoting macrophages [14, 15]. Whether the expression of this protein can be used as a biomarker to select patients for treatment with regorafenib + PD1/PDL1 inhibition requires further investigation.

Considering the pivotal role of TAMs in immunotherapy, numerous strategies have been developed to enhance existing ICB treatments, with both laboratory and clinical studies targeting TAMs. While one primary tactic is the removal of TAMs, their fundamental roles — such as serving as primary phagocytes and antigen-presenting cells — make this approach questionable. Reprogramming TAMs is gaining traction as a potentially more effective strategy to augment the efficacy of immune checkpoint inhibition. For instance, a noteworthy study by Shi et al. demonstrated that in vivo DKK1 blockade successfully reprogrammed TAMs, reinvigorating immune activity within the tumor immune microenvironment and leading to marked tumor regression in a gastric cancer preclinical model [12].

Conclusions

Our findings indicate that joint blockade of vascular endothelial growth factor and programmed death 1 is an effective treatment for a subset of patients with advanced gastric cancer. Furthermore, our study highlights the potential importance of tumor-associated macrophages in mediating resistance, suggesting a direction for future research.

Abbreviations

AGC	Advanced Gastric Cancer
AOI	Area of Illumination
ATTRACTION	2 - Study name
CheckMate	649 - Study name
CPS	Combined Positive Score
CTCAE	Common Terminology Criteria for Adverse Events
ECOG	Eastern Cooperative Oncology Group
GMI	Growth Modulation Index
ICIs	Immune Checkpoint Inhibitors
IHF	Immunohistofluorescence
KEYNOTE	811 - Study name
LENPEM	Lenvatinib Plus Pembrolizumab
NCI	National Cancer Institute
OS	Overall Survival
PD	-1 - Programmed Death-1
PD	-L1 - Programmed Death Ligand-1
PEA	Proximity Extension Assay
PFS	Progression-Free Survival
RECIST 1.1	Response Evaluation Criteria In Solid Tumors, version 1.1
REGOMUNE	Study name involving Regorafenib
REGONIVO	Regorafenib Plus Nivolumab
ROI	Regions of Interest
VEGF	Vascular Endothelial Growth Factor
WTA	Whole Transcriptome Atlas

Supplementary Information

The online version contains supplementary material available at https://doi.org/10.1186/s12943-024-02092-x.

Supplementary Material 1

Supplementary Material 1

Electronic supplementary materialBelow is the link to the electronic supplementary material.Supplementary Material 1

Author contributions

AI, AB, CB and SC conceived and designed the study. IS and LV performed the histological analyses. KS, LJP, JPM, SP, SF, SK, HN, CB, AA, CGR, PAC, AH, MK, provided study material or treated patients. CC and JPG performed the statistical analyses. All authors collected and assembled data. AI, AB, and JPG developed the tables and figures. AI, AB, and JPG conducted the literature search and wrote the manuscript. All authors were involved in the critical review of the manuscript and approved the final version.

Funding

This study was funded by BAYER.

Data availability

No datasets were generated or analysed during the current study.

Declarations

Competing interests

AB and JPG: Employees of Immusmol/Explicyte. AI: Received research grants from Astra Zeneca, Bayer, BMS, Chugai, Merck, MSD, Pharmamar, Novartis, Roche, and received personal fees from BMS, MSD, Merck, Roche, Epizyme, Bayer, Lilly, Roche, and Springworks. The other authors have nothing to disclose.

Ethical approval

This study was approved by a Central Institutional Review Board (Comité de Protection des Personnes Sud-Est II, Lyon, France), according to good clinical practices and applicable laws and regulations. All methods were performed in accordance with the relevant guidelines and regulations. All patients provided written informed consent.

Author details

[1]Department of Medicine, Institut Bergonié, 229 cours de l'Argonne, Bordeaux 33000, France
[2]Explicyte, Bordeaux, France

[3]Department of Gastroenterology and Gastrointestinal Oncology, National Cancer Center Hospital East, Chiba 277-8577, Japan
[4]Department of Oncology, University Hospital Center of Brest, Brest, France
[5]Division of Cancer Immunology, Research Institute/Exploratory Oncology Research and Clinical Trial Center (EPOC), National Cancer Center, Tokyo, Chiba 104-0045, 277-8577, Japan
[6]Bordeaux Population Health Research Center, Univ. Bordeaux, Epicene team, UMR 1219, Inserm, Bordeaux, France
[7]Clinical and Epidemiological Research Unit, INSERM CIC1401, Bordeaux, France
[8]Department of Medicine, Institut Cancerologie Montpellier, Montpellier, France
[9]Department of Medicine, Oncopole, Toulouse, France
[10]Department of Medicine, Centre Leon Bérard, Lyon, France
[11]DITEP, Gustave Roussy, Villejuif, France
[12]Department of Radiology, Institut Bergonié, Bordeaux, France
[13]Department of Pathology, Institut Bertognié, Bordeaux, France
[14]Faculty of Medicine, University of Bordeaux, Bordeaux, France

Received: 19 July 2024 / Accepted: 16 August 2024
Published online: 13 September 2024

References

1. Kang YK, Boku N, Satoh T, Ryu MH, Chao Y, Kato K, Chung HC, Chen JS, Muro K, Kang WK, Yeh KH, Yoshikawa T, Oh SC, Bai LY, Tamura T, Lee KW, Hamamoto Y, Kim JG, Chin K, Oh DY, Minashi K, Cho JY, Tsuda M, Chen LT. Nivolumab in patients with advanced gastric or gastro-oesophageal junction cancer refractory to, or intolerant of, at least two previous chemotherapy regimens (ONO-4538-12, ATTRACTION-2): a randomised, double-blind, placebo-controlled, phase 3 trial. Lancet. 2017;390(10111):2461–71.
2. Janjigian YY, Shitara K, Moehler M, Garrido M, Salman P, Shen L, Wyrwicz L, Yamaguchi K, Skoczylas T, Campos Bragagnoli A, Liu T, Schenker M, Yanez P, Tehfe M, Kowalyszyn R, Karamouzis MV, Bruges R, Zander T, Pazo-Cid R, Hitre E, Feeney K, Cleary JM, Poulart V, Cullen D, Lei M, Xiao H, Kondo K, Li M, Ajani JA. First-line nivolumab plus chemotherapy versus chemotherapy alone for advanced gastric, gastro-oesophageal junction, and oesophageal adenocarcinoma (CheckMate 649): a randomised, open-label, phase 3 trial. Lancet. 2021;398(10294):27–40.
3. Janjigian YY, Kawazoe A, Yañez P, Li N, Lonardi S, Kolesnik O, Barajas O, Bai Y, Shen L, Tang Y, Wyrwicz LS, Xu J, Shitara K, Qin S, Van Cutsem E, Tabernero J, Li L, Shah S, Bhagia P, Chung HC. The KEYNOTE-811 trial of dual PD-1 and HER2 blockade in HER2-positive gastric cancer. Nature. 2021;600(7890):727–30.
4. Voron T, Colussi O, Marcheteau E, Pernot S, Nizard M, Pointet AL, Latreche S, Bergaya S, Benhamouda N, Tanchot C, Stockmann C, Combe P, Berger A, Zinzindohoue F, Yagita H, Tartour E, Taieb J, Terme M. VEGF-A modulates expression of inhibitory checkpoints on CD8+T cells in tumors. J Exp Med. 2015;212(2):139–48.
5. Chen H, Jiang T, Lin F, Guan H, Zheng J, Liu Q, Du B, Huang Y, Lin X. PD-1 inhibitor combined with apatinib modulate the tumor microenvironment and potentiate anti-tumor effect in mice bearing gastric cancer. Int Immunopharmacol. 2021;99:107929.
6. Fukuoka S, Hara H, Takahashi N, Kojima T, Kawazoe A, Asayama M, Yoshii T, Kotani D, Tamura H, Mikamoto Y, Hirano N, Wakabayashi M, Nomura S, Sato A, Kuwata T, Togashi Y, Nishikawa H, Shitara K. Regorafenib Plus Nivolumab in patients with Advanced gastric or colorectal Cancer: an Open-Label, Dose-Escalation, and dose-expansion phase ib trial (REGONIVO, EPOC1603). J Clin Oncol. 2020;38(18):2053–61.
7. Kawazoe A, Fukuoka S, Nakamura Y, Kuboki Y, Wakabayashi M, Nomura S, Mikamoto Y, Shima H, Fujishiro N, Higuchi T, Sato A, Kuwata T, Shitara K. Lenvatinib plus Pembrolizumab in patients with advanced gastric cancer in the first-line or second-line setting (EPOC1706): an open-label, single-arm, phase 2 trial. Lancet Oncol. 2020;21(8):1057–65.
8. Chao J, Fuchs CS, Shitara K, Tabernero J, Muro K, Van Cutsem E, Bang YJ, De Vita F, Landers G, Yen CJ, Chau I, Elme A, Lee J, Özgüroglu M, Catenacci D, Yoon HH, Chen E, Adelberg D, Shih CS, Shah S, Bhagia P, Wainberg ZA. Assessment of Pembrolizumab Therapy for the treatment of microsatellite instability-high gastric or gastroesophageal Junction Cancer among patients in the KEYNOTE-059, KEYNOTE-061, and KEYNOTE-062 clinical trials. JAMA Oncol. 2021;7(6):895–902.
9. Pavlakis N, Sjoquist KM, Martin AJ, Tsobanis E, Yip S, Kang YK, Bang YJ, Alcindor T, O'Callaghan CJ, Burnell MJ, Tebbutt NC, Rha SY, Lee J, Cho JY, Lipton LR, Wong M, Strickland A, Kim JW, Zalcberg JR, Simes J, Goldstein D. Regorafenib for the treatment of Advanced Gastric Cancer (INTEGRATE): a multinational placebo-controlled phase II trial. J Clin Oncol. 2016;34(23):2728–35.
10. Xu J, Zhang Y, Jia R, Yue C, Chang L, Liu R, Zhang G, Zhao C, Zhang Y, Chen C, Wang Y, Yi X, Hu Z, Zou J, Wang Q. Anti-PD-1 antibody SHR-1210 combined with apatinib for Advanced Hepatocellular Carcinoma, gastric, or Esophagogastric Junction Cancer: an Open-label, dose escalation and expansion study. Clin Cancer Res. 2019;25(2):515–23. https://doi.org/10.1158/1078-0432.CCR-18-2484.
11. Saeed A, Park R, Dai J, Al-Rajabi R, Kasi A, Baranda J, Williamson S, Saeed A, Ripp J, Collins Z, Mulvaney K, Shugrue M, Firth-Braun J, Godwin AK, Madan R, Phadnis M, Sun W. Cabozantinib plus Durvalumab in advanced gastroesophageal cancer and other gastrointestinal malignancies: phase ib CAMILLA trial results. Cell Rep Med. 2023;4(2):100916.
12. Shi T, Zhang Y, Wang Y, Song X, Wang H, Zhou X, Liang K, Luo Y, Che K, Wang X, Pan Y, Liu F, Yang J, Liu Q, Yu L, Liu B, Wei J. DKK1 promotes Tumor Immune Evasion and impedes Anti-PD-1 treatment by inducing immunosuppressive macrophages in gastric Cancer. Cancer Immunol Res. 2022;10(12):1506–24.
13. Cousin S, Cantarel C, Guegan JP, Gomez-Roca C, Metges JP, Adenis A, Pernot S, Bellera C, Kind M, Auzanneau C, Le Loarer F, Soubeyran I, Bessede A, Italiano A. Regorafenib-Avelumab combination in patients with microsatellite stable colorectal Cancer (REGOMUNE): a Single-arm, Open-label, phase II trial. Clin Cancer Res. 2021;27:2139–47.
14. El-Rifai W, Moskaluk CA, Abdrabbo MK, Harper J, Yoshida C, Riggins GJ, Frierson HF Jr, Powell SM. Gastric cancers overexpress S100A calcium-binding proteins. Cancer Res. 2002;62(23):6823–6.
15. Phipps KD, Surette AP, O'Connell PA, Waisman DM. Plasminogen receptor S100A10 is essential for the migration of tumor-promoting macrophages into tumor sites. Cancer Res. 2011;71(21):6676–83.

Publisher's note